

DOE-ER40757-097  
UTEXAS-HEP-97-6  
OITS-624  
OSURN-323

## Scalar tau Signal at LEP 2 in models with Gauge Mediated Supersymmetry Breaking

D. A. Dicus<sup>1,2</sup>, B. Dutta<sup>3</sup>, and S. Nandi<sup>4</sup>

<sup>1</sup> *Center for Particle Physics, University of Texas, Austin, TX 78712*

<sup>2</sup> *Department of Physics, University of Texas, Austin, TX 78712*

<sup>3</sup> *Institute of Theoretical Science, University of Oregon, Eugene, OR 97403*

<sup>4</sup> *Department of Physics, Oklahoma State University, Stillwater, OK 74078*

(March, 1997)

### Abstract

In theories with gauge mediated supersymmetry breaking, the scalar tau, ( $\tilde{\tau}_1$ ) is the lightest observable superpartner for part of the parameter space. At LEP 2, the production of such a  $\tilde{\tau}_1$  pair and their subsequent decays give rise to a pair of  $\tau$  leptons plus missing energy from the unobserved gravitinos. The angular distributions of the  $\tau$ 's are different from those arising from the production and decay of W pairs, and thus will constitute an interesting signal for supersymmetry. We also consider  $\tilde{\tau}_1$  pair production in the complementary part of parameter space where the lightest neutralino is lighter than the  $\tilde{\tau}_1$ .  
PACS numbers: 11.30.Pb 12.60.Jv 14.80.Ly

Typeset using REVTeX

In spite of many interesting features of supersymmetric theories, the mechanism of supersymmetry breaking and how it is communicated to the observable sector has been a major area of concern for over a decade. In most of the previous work it has been assumed that the supersymmetry is broken in a hidden sector at a scale of  $\sim 10^{11}$  GeV, and communicated to the observable sector via the gravitational interaction. However, this scenario has a major problem involving flavor changing neutral current (FCNC). This can be avoided if supersymmetry is broken in a hidden sector at a scale  $10^5$  GeV, and communicated to the observable sector by means of the Standard Model (SM) gauge interaction [1]. The number of parameters is also smaller in these gauge mediated models (GMSB) which makes them more predictive. These models have a very distinctive feature, the gravitino is the lightest supersymmetric particle(LSP) and all super particles must ultimately decay to it. This feature gives rise to some new signals in colliders that may be observed in the near future.

One interesting aspect of gauge mediated models is that the role of the next-to-lightest supersymmetric particle (NLSP) can be taken by either the lighter scalar tau ( $\tilde{\tau}_1$ ) or the lightest neutralino. In the past year a lot of work has been done [2–11] in these models motivated in part by the fact that, when the neutralino is the NLSP, the CDF event ( $ee\gamma\gamma$ +missing energy [12]) can be explained. However there is a vast region of parameter space where the lighter stau can be the NLSP and the lightest neutralino is the NNLSP(Next to Next to LSP). Recently, we considered neutralino pair production in these scenarios where the stau is the NLSP and showed that the neutralino pair gives rise to  $4\tau$  + missing energy in the final state without any standard model background [13]. In this paper we look at direct production of stau in the scenarios where the lighter stau is the NLSP as well as in the scenarios where neutralino is the NLSP. In the first case, since the only decay mode available to a lighter stau is to decay into a  $\tau$  and a gravitino, the signal is  $2\tau$  + missing energy. We compare the signal with the background generated from W pair production (each W can decay into a  $\tau$  and a tau neutrino( $\nu_\tau$ )), and show that the angular distribution of the individual  $\tau$ 's will make the signal look very different from the background. For the 2nd case the signal is  $2\tau + 2\gamma$  with missing energy since each stau decays into a neutralino and

a  $\tau$  and the neutralino then decays into a hard photon and a gravitino. So the signal itself can discern the two cases. We also discuss the angular distribution and energy distribution of the decay products in the 2nd case.

In GMSB models the superparticle masses depend on five parameters  $M, \Lambda, n, \tan \beta, \mu$ .  $M$  is the messenger scale,  $M = \lambda \langle s \rangle$ , where  $\langle s \rangle$  is the VEV of the scalar component of the hidden sector superfields, and  $\lambda$  is the Yukawa coupling. The parameter  $\Lambda$  is equal to  $\langle F_s \rangle / \langle s \rangle$ , where  $\langle F_s \rangle$  is the VEV of the auxillary component of  $s$ .  $F_s$  can be  $\sim F$  [14], where  $F$  is the intrinsic SUSY breaking scale. In GMSB models,  $\Lambda$  is taken around 100 TeV, so that the colored superpartners have masses around a TeV or less. The parameter  $n$  is fixed by the choice for the messenger sector. The messenger sector representations should be vector like (for example,  $5 + \bar{5}$  of  $SU(5)$ ,  $10 + \bar{10}$  of  $SU(5)$  or  $16 + \bar{16}$  of  $SO(10)$ ) so that their masses are well above the electroweak scale. They are also chosen to transform as a GUT multiplet in order not to affect the gauge coupling unification in MSSM. This restricts  $n(5 + \bar{5}) \leq 4$ ,  $n(10 + \bar{10}) \leq 1$  in  $SU(5)$ , and  $n(16 + \bar{16}) \leq 1$  in  $SO(10)$  GUT for the messenger sector (one  $10 + \bar{10}$  pair corresponds to  $n(5 + \bar{5})=3$ ). The parameter  $\tan \beta$  is the usual ratio of the up ( $H_u$ ) and down ( $H_d$ ) type Higgs VEVs. The parameter  $\mu$  is the coefficient in the bilinear term,  $\mu H_u H_d$  in the superpotential, while another parameter  $B$  is defined to be the coefficient in the bilinear term,  $B \mu H_u H_d$  in the potential. In general,  $\mu$  and  $B$  depend on the details of the SUSY breaking in the hidden sector. We demand that the electroweak symmetry is broken radiatively which determines  $\mu^2$  and  $B$  in terms of the other parameters of the theory. Thus we are left with five independent parameters,  $M, \Lambda, n, \tan \beta$  and  $\text{sign}(\mu)$ . The soft SUSY breaking gaugino and the scalar masses at the messenger scale  $M$  are given by [1,15]

$$\tilde{M}_i(M) = n g \left( \frac{\Lambda}{M} \right) \frac{\alpha_i(M)}{4\pi} \Lambda. \quad (1)$$

and

$$\tilde{m}^2(M) = 2(n) f \left( \frac{\Lambda}{M} \right) \sum_{i=1}^3 k_i C_i \left( \frac{\alpha_i(M)}{4\pi} \right)^2 \Lambda^2. \quad (2)$$

where  $\alpha_i$ ,  $i = 1, 2, 3$  are the three SM gauge couplings and  $k_i = 1, 1, 3/5$  for SU(3), SU(2), and U(1), respectively. The  $C_i$  are zero for gauge singlets, and  $4/3$ ,  $3/4$ , and  $(Y/2)^2$  for the fundamental representations of SU(3) and SU(2) and  $U(1)_Y$  respectively (with Y defined by  $Q = I_3 + Y/2$ ). Here  $n$  corresponds to  $n(5 + \bar{5})$ .  $g(x)$  and  $f(x)$  are messenger scale threshold functions with  $x = \Lambda/M$ .

We have calculated the SUSY mass spectrum using the appropriate RGE equations [16] with the boundary conditions given by equation (1) and (2), and varying the five free parameters. Although in principle the messenger scale is arbitrary (with  $M/\Lambda > 1$ ), in our analysis we have restricted  $1 < M/\Lambda < 10^4$  and chosen  $\Lambda \sim 100$  TeV. For the messenger sector, we choose  $5 + \bar{5}$  of SU(5), and varied  $n(5 + \bar{5})$  from 1 to 4. In addition to the current experimental bounds on the superpartner masses, the rate for  $b \rightarrow s\gamma$  decay puts useful constraints on the parameter space [6,7,17]. It is found that [6,8] for  $n = 1$  and low values  $\tan\beta$  ( $\tan\beta \leq 25$ ), the lightest neutralino  $\chi_0$  is the NLSP for  $M/\Lambda > 1$ . As  $\tan\beta$  increases,  $\tilde{\tau}_1$  becomes the NLSP for most of the parameter space with lower values of  $\Lambda$ . For  $n \geq 2$ ,  $\tilde{\tau}_1$  is the NLSP even for the low values of  $\tan\beta$  (for example,  $\tan\beta \gtrsim 2$ ), and for  $n \geq 3$ ,  $\tilde{\tau}_1$  is again naturally the NLSP for most of the parameter space. In Tables 1 and 2 we show five sets of spectrum where the lighter stau is the NLSP and five sets where the lightest neutralino is the NLSP. We use these scenarios for detailed calculations.

Let us first discuss the production cross section of the  $\tilde{\tau}_1$  pair in the scenarios 1-5 of Table 1, where the lighter stau is the NLSP. The total cross-sections are given in Table 3 for three LEP2 energies,  $\sqrt{s} = 172, 182$  and  $194$  GeV. Each of the produced  $\tilde{\tau}_1$  will decay into a  $\tau$  and a gravitino with essentially a 100% branching ratio. Thus, from  $\tilde{\tau}_1$  pair production, we obtain final states with two  $\tau$ 's and missing energy. For example, the number of events in scenario 5 for  $\sqrt{s} = 182$  GeV, with  $100pb^{-1}$  luminosity, is 27, and for  $\sqrt{s} = 194$  GeV, with  $250pb^{-1}$  luminosity is 70. The decay,  $\tilde{\tau}_1 \rightarrow \tau\tilde{G}$  is fast enough so that it takes place inside the detector. (If  $\sqrt{F}$  is much larger than a few 1000 TeV [18], then  $\tilde{\tau}_1$  will decay outside the detector. In that case the signal will be 2 heavy charged particles passing through the detector).

There is a considerable background from W production, where each W decays into a  $\tau$  and a neutrino. However since the staus are scalar particles, their angular distribution is different from the W distribution. This shows up in the individual  $\tau$  angular distributions. In Figure 1 we show these angular distributions of the  $\tau$ s. As expected the angular distribution of the  $\tau$  coming from stau decay is basically flat; the same distribution from W decay has significant  $\theta$  dependence (as measured from the beam direction). Consequently, the signal is almost twice the background for  $\tau^-$  when  $\cos\theta$  is negative. The opposite thing happens for  $\tau^+$  i.e the positive values of the  $\cos\theta$  regions need to be searched for  $\tau^+$  in order to extract the signal.

The information in Fig.1, and its mirror image for the  $\tau$  of the other charge, is made more precise in Table 4 where we give the fraction of events that should be found in each bin of width 0.2 in  $\cos\theta_+$  and in  $\cos\theta_-$ .

Figure 2 shows the distribution in the angle between the two tau is very similar in stau or W production.

In Table 3 we also show the cross-section for charged Higgs production in a usual SUSY model. The charged Higgs in the GMSB model are too heavy to be produced at LEP 2 but in other models they could be light and, because they decay into a  $\tau + \nu_\tau$  with essentially 100% branching ratio if  $\tan\beta$  is greater than 2, and because they are produced with the same angular distribution as the stau, they are indistinguishable from stau production of the same mass in GMSB except through the total production rate which is a little larger than for stau. For example the number of events, when the charged Higgs mass is comparable to the lighter stau mass in the scenario 5, is 34 for  $\sqrt{s} = 182$  GeV with  $100pb^{-1}$  luminosity and is 89 for  $\sqrt{s} = 194$  GeV with  $250pb^{-1}$  luminosity. So if a two tau signal is observed at LEP 2, with a limited number of events so that the difference in the production rate is not sufficient to discern between these two models, then other signals, such as 4  $\tau +$  missing energy from neutralino pair production [13], will have to be used. We note here that in the case of charged Higgs pair productions, with subsequent decay into  $\tau$  will have similar angular distribution as those coming from stau. Thus, the signal for the charged Higgs can

also be distinguished from the W-background using the distribution shown in Fig1.

We now discuss the scenarios of Table 2 where the lightest neutralino is the NLSP. In Table 5 we give the cross section where staus are produced. The signal in this case is different than the signal in the case where stau is the NLSP; here each stau will decay into a  $\tau$  and a neutralino and the neutralino will then decay into a gravitino and a photon giving rise to  $2 \tau + 2 \gamma +$  missing energy in the final state. The photons are hard and they can be easily seperated from bremsstrahlung. The number of events in scenario 6 for  $\sqrt{s} = 182$  GeV, with  $100pb^{-1}$  luminosity, is 30 and for  $\sqrt{s} = 194$  GeV , with  $250pb^{-1}$  luminosity is 77. Since the neutralino is the NLSP in these scenarios, they can be pair produced more easily than the staus. Consequently the signal of 2 photons(hard) and missing energy in the final state coming from the neutralino decays could be used to discover SUSY and a detailed analysis of the stau production will then give information on particular models.

In Figure 3 we plot the angular distributions of the one of the emitted photons and the distribution of the angle between the two emitted photons. The angular distribution of the single photon is almost isotropic while the angular distribution of the angle between the photons has  $\theta$  dependence; the distribution is large when  $\cos\theta$  is negative. The angular distribution of one of the  $\tau$ , or of the angle between the two  $\tau$  looks very similar to Fig. 3. In Fig. 4 we show the angle between a tau and a photon from the same stau decay and between a tau and a photon which come from opposite stau decays. In Fig. 5, we also plot the energy distributions of the decay products, ie., the total missing energy, the energy of one of the photons and the energy of one of the  $\tau$ 's. Since the massive neutralino carries more than half of the energy of the lighter stau, each gravitino carries more than 1/6 of the total energy and the total missing energy distribution becomes a maximum at more than 1/3 of the beam energy. The energy distribution for the  $\tau$ 's and photons maximize at much smaller energy.

In conclusion, we have discussed the production of scalar staus and their decay modes in gauge mediated models in the scenarios where the lighter stau is the NLSP as well as in the scenarios where the neutralino is the NLSP. We have discussed the background for the

individual cases and have shown how the signal can be extracted from the SM background. We also have noted that the charged Higgs in the supergravity models can have signatures that are almost identical to that of the stau in these models so that observation of this signal is a sign of new physics but not necessarily of gauge mediated supersymmetry breaking.

After finishing this work, we came across a preprint by S. Ambrosanio, G. D. Kribs and S. P. Martin, hep-ph/9703211, which has partial overlap with our work.

We are very grateful to David Strom of OPAL collaboration for many discussions. Part of this work has been done when one of us (S.N.) was on sabbatical leave at the University of Texas at Austin. He wishes to thank Duane Dicus of the Center for Particle Physics for very warm hospitality and support during his stay there. This work was supported in part by the US Department of Energy Grants No. DE-FG013-93ER40757, DE-FG02-94ER40852, and DE-FG03-96ER-40969.

## REFERENCES

- [1] M. Dine and A. Nelson, *Phys. Rev.* **D47**, 1277 (1993); M. Dine, A. Nelson and Y. Shirman, *Phys. Rev.* **D51**, 1362 (1995); M. Dine, A. Nelson, Y. Nir and Y. Shirman, *Phys. Rev.* **D53**, 2658 (1996); M. Dine, Y. Nir and Y. Shirman, preprint SCIPP-96-30, hep-ph/9607397; R. N. Mohapatra and S. Nandi, hep-ph/9702291.
- [2] S. Dimopoulos, M. Dine, S. Raby and S. Thomas, *Phys. Rev. Lett.* **76**, 3494 (1996); S. Ambrosanio, G. L. Kane, G. D. Kribs, S. P. Martin and S. Mrenna, *Phys. Rev. Lett.* **76**, 3498 (1996);
- [3] D. R. Stump, M. Wiest and C.P. Yuan, *Phys. Rev.* **D54**,1936, (1996).
- [4] K.S. Babu, C. Kolda and F. Wilczek, *Phys. Rev. Lett.* **77**, 3070, (1996).
- [5] S. Ambrosanio, G. L. Kane, G. D. Kribs, S. P. Martin and S. Mrenna, *Phys. Rev.* **D54**, 5395, (1996); hep-ph/9607414.
- [6] S. Dimopoulos, S. Thomas and J.D. Wells, hep-ph/9609434.
- [7] H. Baer, M. Brhlik, C.-H. Chen and X. Tata, hep-ph/9610358.
- [8] J. Bagger, D. Pierce, K. Matchev and R.-J.Zhang, hep-ph/960944.
- [9] A. Riotto, O. Tornkvist and R.N. Mohapatra, *Phys. Lett.* **B 388**, 599, (1996).
- [10] G. Bhattacharyya, A. Romanino; hep-ph/9611243.
- [11] A. Ghosal, A. Kundu, B. Mukhopadhyaya; hep-ph/9612321.
- [12] S. Park, representing the CDF collaboration, “Search for New Phenomena in CDF,” in *10th Topical Workshop on Proton-Antiproton Collider Physics*, ed. by R. Raja and J. Yoh (AIP Press, New York, 1995), report FERMILAB-CONFE-95/155-E.
- [13] D. A. Dicus, B. Dutta and S. Nandi, hep-ph/9701341, to appear in *Phys. Rev. Lett.*
- [14] K. Intriligator and S. Thomas, hep-ph/9603158.

- [15] S. Dimopoulos, G.F. Giudice and A. Pomarol, preprint CERN-TH/96-171, hep-ph/9607225; S. P. Martin, hep-ph/9608224.
- [16] V. Barger, M. Berger, P. Ohmann, and R. J. N. Phillips, Phys. Rev.**D51**, 2438 (1995), and references therein.
- [17] N. G. Deshpande, B. Dutta and S. Oh, hep-ph/9607397.
- [18] For example, see Dimopoulos et. al. in Ref. 2.

## TABLE CAPTIONS

Table 1 : Mass spectrum for the superpartners in some scenarios where the lighter stau is the NLSP. Note that the 1st and 2nd generation superpartner masses are almost same.

Table 2 : Mass spectrum for the superpartners in some scenarios where the lightest neutralino is the NLSP.

Table 3 : For each scenario in Table 1 and three beam energies the first line gives the total cross section for stau pair production, while the 2nd line gives the total cross section for charged Higgs production.

Table 4 : The double angular distribution of the two tau. The numbers are the per cent of total events where each tau is in a bin in  $\cos\theta$  of width 0.2. The first number in each bin is for  $\tau$  from  $e^+e^- \rightarrow \tilde{\tau}_1\tilde{\tau}_1 \rightarrow \tau\tau\tilde{G}\tilde{G}$ ; the number in brackets is for  $\tau$  from  $e^+e^- \rightarrow WW \rightarrow \tau\tau\nu_\tau\nu_\tau$ . The table is symmetric about the complementary diagonal, ie., the numbers for  $(\cos\theta_+, \cos\theta_-)$  are the same as those for  $(-\cos\theta_-, -\cos\theta_+)$ .

Table 5 : For each scenario in Table 2 and three beam energies the total cross section for stau pair production is shown.

## FIGURE CAPTIONS

Fig. 1 : The angular distribution of  $\tau^-$ , relative to the electron beam axis, from the stau decay (dashed line) and from W decay (solid line). The distribution of the  $\tau^+$  is the mirror image of this graph.

Fig. 2 : The relative number of events as a function of the angle between the  $\tau^+$  and the  $\tau^-$ . The dashed line corresponds to the  $\tau$ s from the stau decay and the solid line corresponds to the  $\tau$ s from the W decay.

Fig. 3 : The angular distribution of one of the photons (dashed line) and the angle between the two photons (solid line) from neutralino decay, when the neutralino is the NLSP.

Fig. 4 : The angular distribution between a  $\tau$  and a photon. The solid line corresponds to the  $\tau$  and the photon from the same stau and the dashed line corresponds to the same particles from opposite stau.

Fig. 5 : The distribution of the missing energy (solid line), the energy of one of the photons (dashed), and the energy of one of the  $\tau$  (dot-dashed), when the neutralino is the NLSP.

Table 1

|                          | Scenario 1  | Scenario 2   | Scenario 3   | Scenario 4   | Scenario 5   |
|--------------------------|---|--|--|--|--|
| masses<br>(GeV)          | $\Lambda = 63.7 \text{ TeV},$<br>$n=1, M = 4\Lambda$<br>$\tan \beta=31.5$ | $\Lambda = 33 \text{ TeV},$<br>$n=2, M = 20\Lambda$<br>$\tan \beta=20$ | $\Lambda = 60 \text{ TeV},$<br>$n=1, M = 10\Lambda$<br>$\tan \beta=31.5$ | $\Lambda = 59.7 \text{ TeV},$<br>$n=1, M = 10\Lambda$<br>$\tan \beta=28.5$ | $\Lambda = 28 \text{ TeV},$<br>$n=2, M = 40\Lambda$<br>$\tan \beta=18$ |
| $m_h$                    | 121   | 117  | 120  | 120  | 114  |
| $m_{H^\pm}$              | 366   | 318  | 356  | 364  | 278  |
| $m_A$                    | 357   | 308  | 347  | 355  | 266  |
| $m_{\chi^0}$             | 85  | 87   | 80   | 80   | 72   |
| $m_{\chi^1}$             | 158   | 156  | 149  | 148  | 128  |
| $m_{\chi^2}$             | 350   | 286  | 345  | 343  | 249  |
| $m_{\chi^3}$             | 364   | 309  | 358  | 356  | 275  |
| $m_{\chi^\pm}$           | 157,367   | 155,312  | 149,361  | 127,277  | 158,367  |
| $m_{\tilde{\tau}_{1,2}}$ | 74,249  | 73,192   | 65,240   | 74,236   | 65,167   |
| $m_{\tilde{e}_{1,2}}$    | 120,236   | 96,184   | 116,225  | 115,224  | 85,159   |
| $m_{\tilde{t}_{1,2}}$    | 664,727   | 515,588  | 607,673  | 605,672  | 432,505  |
| $m_{\tilde{b}_{1,2}}$    | 698,740   | 558,586  | 641,686  | 643,683  | 472,497  |
| $m_{\tilde{u}_{1,2}}$    | 737,765   | 580,601  | 683,710  | 679,709  | 490,508  |
| $m_{\tilde{d}_{1,2}}$    | 735,769   | 580,606  | 681,715  | 678,711  | 490,514  |
| $m_{\tilde{g}}$          | 565   | 587  | 533  | 530  | 498  |
| $\mu$                    | -343  | -278   | -337   | -336   | -240   |

Table 2

|                          | Scenario 6   | Scenario 7   | Scenario 8   | Scenario 9  | Scenario 10   |
|--------------------------|--|--|--|---|---|
| masses<br>(GeV)          | $\Lambda = 42 \text{ TeV},$<br>$n=1, M = 60\Lambda$<br>$\tan \beta=21$ | $\Lambda = 44 \text{ TeV},$<br>$n=1, M = 80\Lambda$<br>$\tan \beta=18$ | $\Lambda = 41 \text{ TeV},$<br>$n=1, M = 1000\Lambda$<br>$\tan \beta=15$ | $\Lambda = 38 \text{ TeV},$<br>$n=1, M = 800\Lambda$<br>$\tan \beta=12$ | $\Lambda = 42 \text{ TeV},$<br>$n=1, M = 1200\Lambda$<br>$\tan \beta=8$ |
| $m_h$                    | 112  | 113  | 111  | 109   | 109   |
| $m_{H^\pm}$              | 280  | 300  | 296  | 277   | 316   |
| $m_A$                    | 268  | 290  | 285  | 265   | 306   |
| $m_{\chi^0}$             | 54   | 57   | 53   | 48  | 53  |
| $m_{\chi^1}$             | 98   | 104  | 96   | 87  | 98  |
| $m_{\chi^2}$             | 255  | 270  | 263  | 244   | 274   |
| $m_{\chi^3}$             | 272  | 286  | 281  | 263   | 293   |
| $m_{\chi^\pm}$           | 98,275   | 290,103  | 284,96   | 266,86  | 96,295  |
| $m_{\tilde{\tau}_{1,2}}$ | 62,174   | 73,180   | 78,171   | 77,157  | 90,171  |
| $m_{\tilde{e}_{1,2}}$    | 89,164   | 92,172   | 92,165   | 86,154  | 94,170  |
| $m_{\tilde{t}_{1,2}}$    | 419,497  | 432,515  | 377,472  | 446,355   | 380,483   |
| $m_{\tilde{b}_{1,2}}$    | 442,473  | 484,512  | 416,442  | 391,412   | 448,432   |
| $m_{\tilde{u}_{1,2}}$    | 466,485  | 485,506  | 436,457  | 406,425   | 445,467   |
| $m_{\tilde{d}_{1,2}}$    | 465,492  | 464,492  | 436,464  | 406,432   | 445,474   |
| $m_{\tilde{g}}$          | 374  | 392  | 366  | 339   | 375   |
| $\mu$                    | -244   | -259   | -253   | -233  | -375  |

Table 3

| Scenario 1 | $\sqrt{s} =$<br>172(GeV) | 182              | 194              |
|------------|--------------------------|------------------|------------------|
| 1          | 0.117 pb<br>(0.152) pb   | 0.155<br>(0.198) | 0.186<br>(0.235) |
| 2          | 0.132<br>(0.169)         | 0.169<br>(0.214) | 0.198<br>(0.248) |
| 3          | 0.246<br>(0.322)         | 0.267<br>(0.344) | 0.279<br>(0.355) |
| 4          | 0.117<br>(0.152)         | 0.155<br>(0.198) | 0.186<br>(0.235) |
| 5          | 0.250 pb<br>(0.322) pb   | 0.270<br>(0.344) | 0.283<br>(0.356) |
| eeWW       | 0.177                    | 0.212            | 0.225            |

Table 4

| $\cos\theta_+$ | $\cos\theta_-$ |                |                |                |                |                |                |                |                |                |
|----------------|----------------|----------------|----------------|----------------|----------------|----------------|----------------|----------------|----------------|----------------|
|                | -0.9           | -0.7           | -0.5           | -0.3           | -0.1           | 0.1            | 0.3            | 0.5            | 0.7            | 0.9            |
| -0.9           | 0.42<br>(0.37) | 0.51<br>(0.57) | 0.62<br>(0.88) | 0.71<br>(1.28) | 0.80<br>(1.73) | 0.91<br>(2.32) | 0.98<br>(2.94) | 1.04<br>(3.45) | 1.09<br>(3.58) | 1.06<br>(2.67) |
| -0.7           | 0.51<br>(0.30) | 0.63<br>(0.45) | 0.75<br>(0.69) | 0.86<br>(1.00) | 0.96<br>(1.40) | 1.08<br>(1.92) | 1.16<br>(2.47) | 1.19<br>(3.08) | 1.18<br>(3.51) |                |
| -0.5           | 0.62<br>(0.26) | 0.75<br>(0.38) | 0.88<br>(0.56) | 1.02<br>(0.82) | 1.11<br>(1.16) | 1.20<br>(1.57) | 1.23<br>(2.05) | 1.27<br>(2.55) |                |                |
| -0.3           | 0.71<br>(0.21) | 0.86<br>(0.32) | 1.02<br>(0.47) | 1.13<br>(0.68) | 1.23<br>(0.92) | 1.29<br>(1.26) | 1.30<br>(1.61) |                |                |                |
| -0.1           | 0.80<br>(0.18) | 0.96<br>(0.27) | 1.11<br>(0.42) | 1.23<br>(0.55) | 1.30<br>(0.76) | 1.31<br>(0.99) |                |                |                |                |
| 0.1            | 0.91<br>(0.16) | 1.08<br>(0.23) | 1.20<br>(0.38) | 1.29<br>(0.45) | 1.31<br>(0.58) |                |                |                |                |                |
| 0.3            | 0.98<br>(0.15) | 1.16<br>(0.21) | 1.28<br>(0.29) | 1.30<br>(0.35) |                |                |                |                |                |                |
| 0.5            | 1.04<br>(0.15) | 1.19<br>(0.19) | 1.27<br>(0.23) |                |                |                |                |                |                |                |
| 0.7            | 1.09<br>(0.15) | 1.18<br>(0.17) |                |                |                |                |                |                |                |                |
| 0.9            | 1.06<br>(0.15) |                |                |                |                |                |                |                |                |                |

Table 5

| Scenarios | $\sqrt{s} =$          |                       |                       |
|-----------|-----------------------|-----------------------|-----------------------|
|           | 172(GeV)              | 182                   | 194                   |
| 6         | 0.293 pb              | 0.307                 | 0.312                 |
| 7         | 0.132                 | 0.169                 | 0.198                 |
| 8         | $7.22 \times 10^{-2}$ | 0.114                 | 0.151                 |
| 9         | $8.54 \times 10^{-2}$ | 0.127                 | 0.162                 |
| 10        | -                     | $4.39 \times 10^{-3}$ | $4.04 \times 10^{-2}$ |

# FIGURES

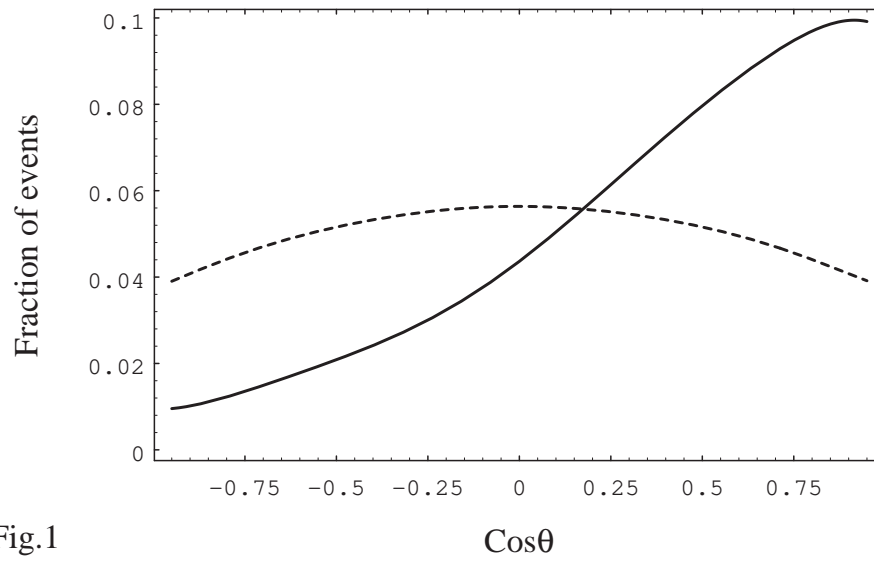


Fig.1

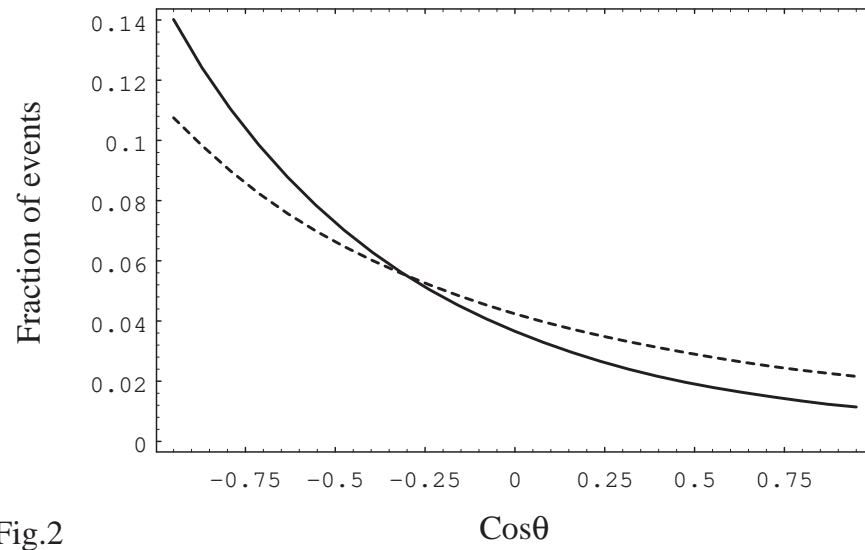


Fig.2

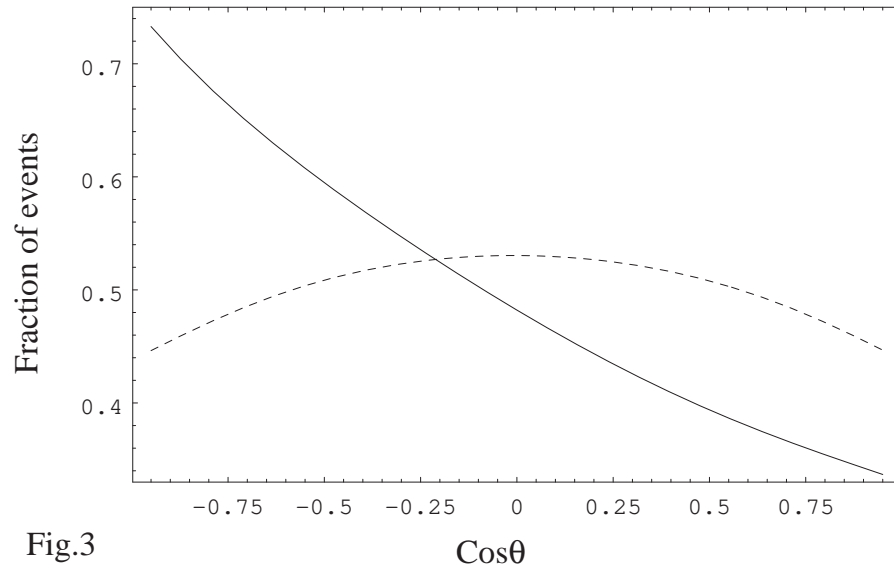


Fig.3

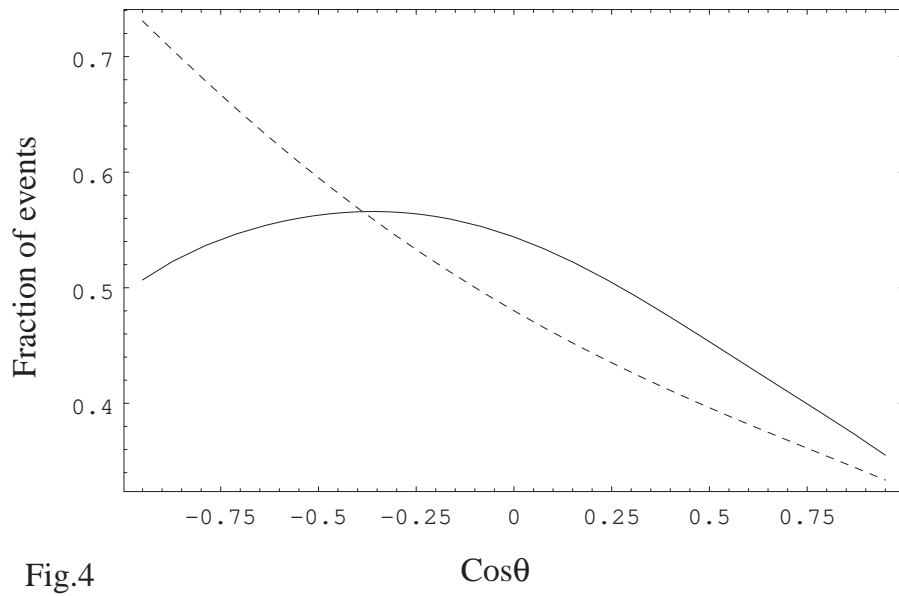


Fig.4

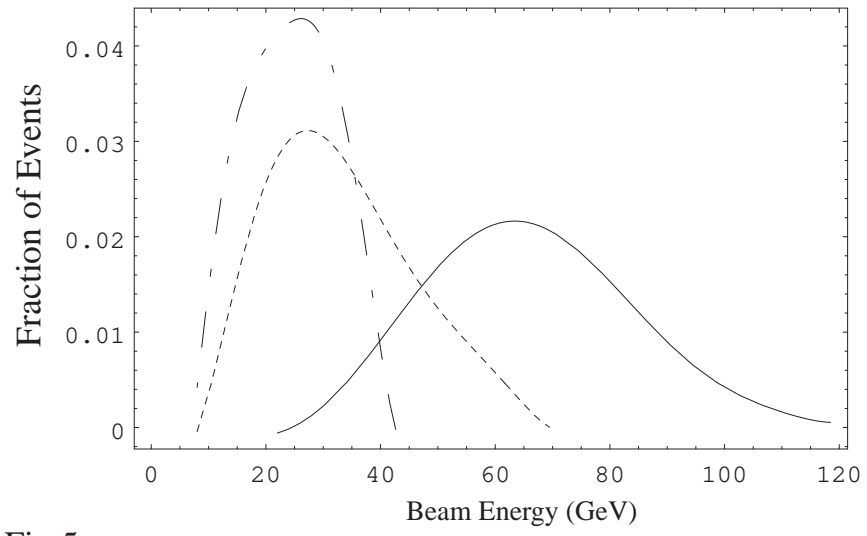


Fig.5